DEEP DECOUPLING OSCILLATIONS OF THE OCEANIC THERMOHALINE CIRCULATION

Michael Winton

Department of Atmospheric Sciences
University of Washington
Seattle, Washington 98195

I. Introduction

The polar ice and ocean sediment cores contain a record of large and sudden climate changes around the North Atlantic Ocean. Evidence for ocean circulation changes occurring synchronously with the terrestrial climate changes has been found in forams from sediment cores which show colder sea surface temperatures and increased deep nutrient levels during the cold Younger Dryas period (Boyle and Keigwin, 1987). The increased nutrients have been interpreted as evidence that North Atlantic Deep Water formation was reduced during the Younger Dryas. A natural conclusion is that such a reduction would have contributed to the cold climate by diminished importation of heat to high, northern hemisphere latitudes. The ^{18}O record from the Greenland ice cores reveals that similar climate oscillations with 500 to 2,000 year warm periods separating the cold periods occurred frequently during the last glaciation (Johnson et al., 1992). These "interstadials" began with abrupt warmings (within decades) followed by gradual or stepwise coolings. Broecker et al. (1990) have suggested that variability of the salinity of the Atlantic Ocean caused by melting ice sheets and water vapor export from the Atlantic forces oscillations in the thermohaline overturning.

Winton and Sarachik (1993, WS hereafter) use a simplified ocean general circulation model to show that internal thermohaline oscillations can result from strong *steady* forcing with high latitude freshening. They refer to these oscillations as deep decoupling oscillations because they involve the periodic failure and reestablishment of deep overturning which accompanies the formation and removal of a high latitude halocline. The phase of the oscillation when deep circulation and convection are active (inactive) is termed the *coupled* (*decoupled*) phase. The deep ocean heat balance between downward diffusion of heat and inflow of cold water from a deep convecting plume which prevails in steady, thermally direct, solutions is never attained in

NATO ASI Series, Vol. I 12
Ice in the Climate System
Edited by W. Richard Peltier

the oscillating solutions. Advective cooling dominates during the coupled phases, causing a decline in basin average temperature, while diffusive heating dominates during the warming decoupled phases. Also associated with the oscillations are large variations in poleward heat transport with a sharp rise at the beginning of the deep coupled phase followed by a gradual reduction and then a sharp reduction to initiate the deep decoupled phase. The results reported in WS raise the possibility that the climatic variations seen in the paleo-record could be due, at least in part, to internal thermohaline oscillations rather than variability in external forcing.

Convective variablity was identified as essential to this kind of oscillation by Marotzke's experiments with a two dimensional model (Marotzke, 1989). He found that an impulsive freshening at high latitudes led to a smooth transition to a steady reversed (thermally indirect) circulation in a model without a convective adjustment but induced oscillations when the convective adjustment was added. Many numerical model simulations have similarly shown considerable sensitivity to surface freshenening through the formation of a halocline over a previously convecting region (the so called *halocline catastrophe*). Surface cooling of the warm poleward flowing branch of a thermally direct meridional cell creates the gravitationally unstable condition which leads to convection. We expect that some amount of surface freshening will be able to overcome this destabilizing effect and eliminate convection. The conceptual challenge presented by the oscillations found under steady forcing in WS is as follows: assuming that the stabilizing effect of surface freshening has dominated the destabilizing effect of upward heat flux at some point to establish a halocline at high latitude, what changes occur to favor thermal destabilization and eventually restart convection?

The answer to this question, for the low amplitude oscillations of WS, was indicated by the "U" shaped evolution of polar region salinity during the decoupled phase -- midway through this phase the halocline ceased strengthening and began weakening. This was shown to be the result of shallow convection (which was maintained in confined areas throughout the decoupled phase) deepening as the deep ocean warmed, spinning up a preexisting thermally direct overturning which imported more heat and salt into the sinking region. The polar region salinity curve for stronger forcing showed a sudden and sharp increase to terminate a decoupled phase with no polar ocean convection. When the forcing was increased still further, high frequency (decadal) variability appeared in polar ocean salinity and convection during the decoupled phase.

In the present study the last two types of behaviors are investigated in more detail. A numerical model which is similar to that of WS but which uses a more conventional formulation of the momentum equation and a standard approximation to the equation of state is used. The choices of model formulation, parameters, and forcing made here yield a range of oscillating solutions

with no polar ocean convection during the decoupled phase. These choices were not made to simulate realistic conditions but rather to isolate specific behaviors. Our object is to understand the mechanism for the break down of the halocline in the absence of a thermally direct convecting cell.

II. The Model

In order to model variability occurring over hundreds to thousands of years, it is necessary to use long timesteps. The primitive equations contain physics for fast barotropic and internal gravity waves which limits the timestep to hours in a coarse resolution model. These waves can be filtered by leaving the time dependent terms out of the momentum equation. This approach was used by Colin de Verdiere (1988, 1989) who obtained circulations and sensitivities similar to those of the primitive equation studies with such a model. A similar model using Rayleigh friction and a parameterized boundary condition to enforce no normal flow was used in WS. The current model employs Laplacian friction and a no slip boundary condition as in the Colin de Verdiere model. The model equations are:

$$f\mathbf{k}\times\mathbf{v} = -\frac{\nabla P}{\rho_0} + A\nabla^2\mathbf{v} + \mathbf{F} \tag{1a}$$

$$0 = \frac{-1}{\rho_0}\frac{\partial P}{\partial z} - \frac{\rho g}{\rho_0} \tag{1b}$$

$$\nabla\cdot\mathbf{v} + \frac{\partial w}{\partial z} = 0 \tag{1c}$$

$$\frac{\partial T}{\partial t} + \mathbf{v}\cdot\nabla T + w\frac{\partial T}{\partial z} = k_v\frac{\partial^2 T}{\partial z^2} + k_h\nabla^2 T + Q_T \tag{1d}$$

$$\frac{\partial S}{\partial t} + \mathbf{v}\cdot\nabla S + w\frac{\partial S}{\partial z} = k_v\frac{\partial^2 S}{\partial z^2} + k_h\nabla^2 S + Q_S \tag{1e}$$

$$\rho = \rho(T,S,P) \tag{1f}$$

where f is the Coriolis parameter, $\mathbf{v}$ is the horizontal velocity vector, w is vertical velocity, T is potential temperature, S is salinity, ρ is potential density, P is pressure, A is the horizontal viscocity, k_v is the vertical mixing coefficient, and k_h is the horizontal mixing coefficient. k_v is set to a large value between grid points where density decreases with height (convective

adjustment). Two equations of state are used in this study: (1) a third order polynomial approximation to the UNESCO equation of state introduced by Cox and Bryan (1972) and included in the GFDL model code; and (2) a linear equation with coefficients for T=4°C, S=35 psu, and P=2000 decibars. The linear equation of state is:

$$\rho(T,S)=0.78\cdot S-0.15\cdot T. \tag{1f'}$$

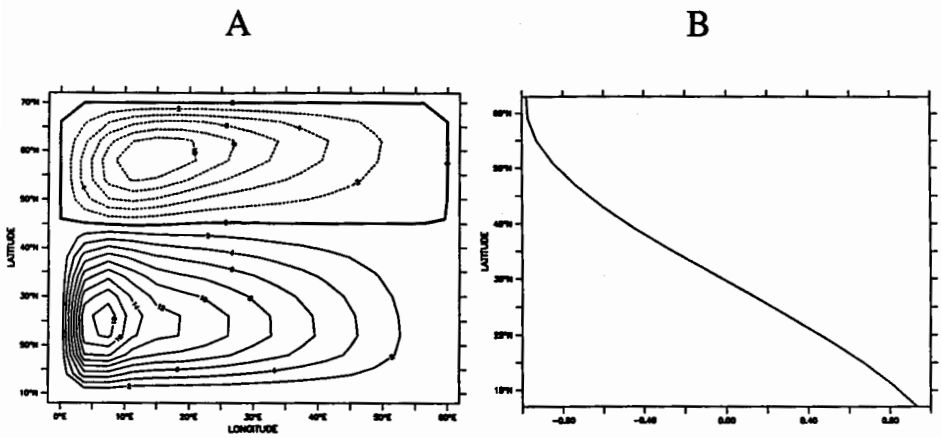

Figure 1: Boundary conditions: (a) steady barotropic stream function resulting from the zonal wind stress pattern (10^6 m^3sec^{-1}), and (b) reference salinity fluxes expressed as equivalent $m\cdot yr^{-1}$ of evaporation minus precipitation at 1 m^3 per 35 kg salt. Negative numbers correspond to a freshening of the surface.

The equations are solved in a 60 degree wide sector of 4 km depth running from 10°N to 70°N in thin shell, spherical coordinates. There are 16 vertical levels, 3.75° zonal resolution, and 4° meridional resolution. The surface forcing is applied to the top 50 m grid layer as follows:

$$\mathbf{F}=\frac{F_w(\varphi)}{\rho_0}\cdot\frac{H(50+z)}{50m}\mathbf{i} \tag{2a}$$

$$Q_T=\frac{(T_a(\varphi)-T(z=25m))}{\tau}\cdot H(50+z) \tag{2b}$$

$$Q_S=F_s(\varphi)\cdot\frac{H(50+z)}{50m} \tag{2c}$$

where H is the Heaviside step function, F_w is the surface wind stress, **i** is the unit vector in the eastward direction, T_a is the surface restoring temperature, and F_s is the surface salt flux. Parameter values for the model are as follows: $A = 2.5 \cdot 10^9$ cm^2·sec^{-1}, $k_v = 0.5$ cm^2·sec^{-1}, $k_h = 10^7$ cm^2·sec^{-1}, $\tau = 61$ days. The restoring temperatures vary between -1.9 °C and 24.1 °C and are given by the formula: $T_a(\varphi) = 43 \cdot cos\varphi - 18$. The zonal wind stress gives the steady barotropic stream function depicted in Fig. 1a. Fig. 1b shows the reference salinity fluxes. The freshening is applied more evenly to the high latitude ocean than in WS, and net evaporation is restricted to latitudes south of 35°N (as opposed to 40°N in WS).

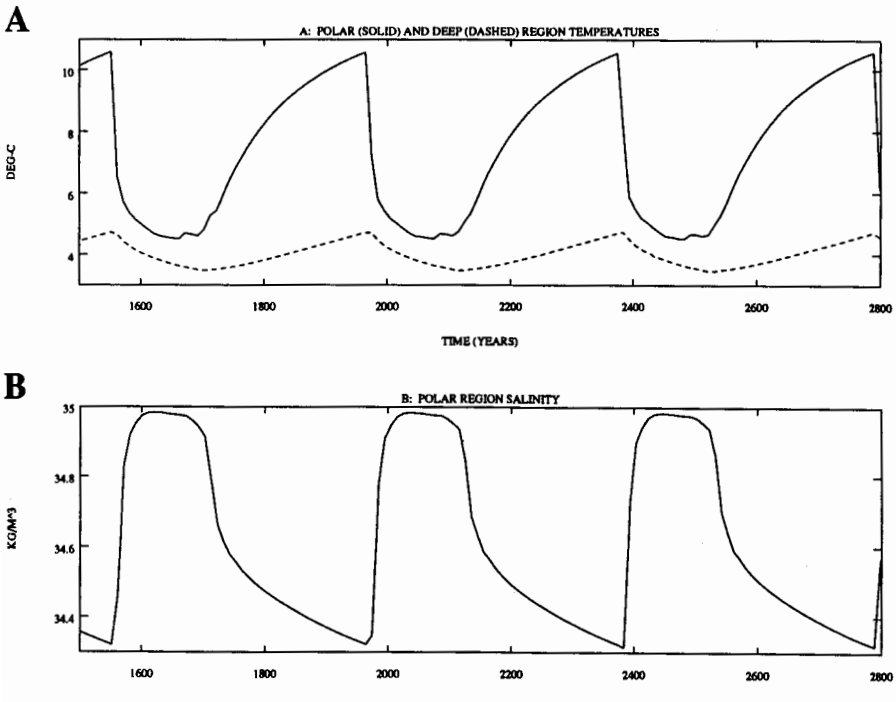

Figure 2: Oscillations induced with 1.35 times the reference salinity forcing: (a) temperature of polar (54°N to 70°N, above 1100 m, solid line) and deep (below 1100 m, dashed line) regions; (b) salinity of polar region.

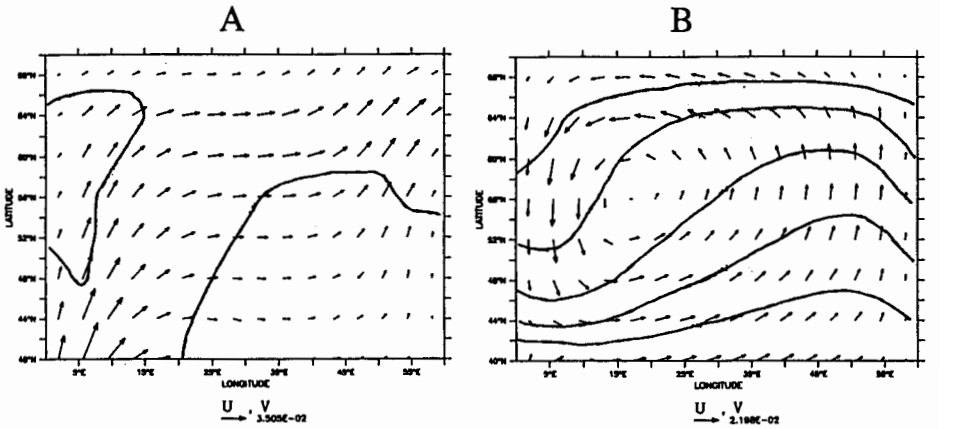

Figure 3: Circulation in the upper subpolar ocean during coupled and decoupled phases of the oscillation. (a) The halocline edge, defined as the region where salinity at the second level (87.5 m) is 0.2 kg·m^{-3} in excess of that at the first level (25 m), is plotted over the 87.5 m circulation during the coupled phase. (b) Contours of temperature at 87.5 m plotted over the circulation during the decoupled phase (contours vary from 14°C in the south to 6°C in the north at 2°C intervals).

III. Deep Decoupling Oscillations

When the high latitude freshening is applied with sufficient strength the model solutions become oscillatory. Figure 2 shows a sequence of 400 year period oscillations in polar (54°N to 70°N, above 1100 m) and deep (below 1100 m) region temperatures and polar region salinity with 1.35 times the reference salt fluxes. During the decoupled phase, deep overturning has switched off and heat diffuses downward warming the basin. In the coupled phase, vigorous deep overturning cools the basin advectively. The amplitude of the deep temperature signal is about 1.25°C while the polar region temperature varies by about 6°C. Although the deep overturning is switching on and off, the most active region in the oscillation is the shallow high latitude ocean. The salinity of this region declines during the decoupled phase, as expected from the increased residence time of water parcels in a region of freshening, but rises suddenly and sharply at the flush (the transition to the coupled phase). No convection is present at high latitudes during the decoupled phase. With lesser forcing (1.3 times reference salt fluxes) oscillations were observed with a "U" shape in polar salinity over the decoupled period intermingled with shorter period, sharp salinity rise oscillations. The "U" shaped oscillations maintained shallow convection and intermediate water formation near the eastern boundary at high latitudes over the decoupled phases. The sharp salinity rise oscillations have some weak

sinking at high latitudes in the decoupled phases but it is not strong enough to appear in the meridional stream function.

The overturning weakens progressively as the basin cools and the associated meridional pressure gradients weaken during the coupled phase of the 1.35 times salt flux oscillations. The conversion of meridional pressure gradients into the zonal pressure gradients with geostrophic meridional flow which comprise the overturning is established by long Rossby waves emanating from the eastern boundary. The reader is referred to Colin de Verdiere (1989) for a discussion of this spin up process. The layer of warm water advected into the polar region also becomes cooler and so there is a reduction of upward heat flux through the polar ocean surface. Halocline forms where this heat flux cannot overcome the surface freshening to maintain convection. In Fig. 3a the halocline has advanced from the southeast and from the western boundary, reducing convective heat loss from the current which passes from the western boundary current to the sinking region in the northeast corner of the basin. The water warms rapidly just beneath this halocline even though there is advective cooling at greater depth. This accounts for the slight increase in polar region temperature prior to the shutoff of the deep overturning (the shutoff is marked by the minimum in deep region temperature). The water in the downward branch of the deep overturning becomes lighter through freshening *and* warming. The zonal, west to east jet of Fig. 3a is a thermal wind circulation due to the sharply decreasing temperatures toward the pole. During the coupled phase the water column north of this jet warms as the growing halocline reduces convective heat loss and the water column to the south cools reducing the intensity of the jet and increasing the residence time of parcels in the polar region where they are exposed to surface freshening. Thus the halocline formation and the weakening circulation are mutually reinforcing processes.

The high latitude circulation is dramatically altered by the presence of a halocline. The wind driven circulation is trapped near the surface of the newly stable water column. In Fig. 3b, the cyclonic wind driven circulation (see Fig. 1a) is now evident at shallow levels. This circulation brings heat northward on its eastern side where it is lost diffusively through the cold upper halocline to the atmosphere. The core of this warm plume is centered in the lower halocline at about 300 m. This plume cools as it makes its cyclonic circuit and so on the western side of the gyre the surface heat flux is downward. The horizontal circulation depicted in Fig. 3b replaces the deep overturning as the primary mode of transport for both heat and salt into high latitudes. Even though the polar region is now warmer than at the end of the coupled phase, the poleward heat transport and heat loss through the surface is reduced because diffusive mixing is less efficient than convection at bringing the heat to the surface. Eventually convection breaks out above the warm plume in the northeast part of the basin (at 60°N, 48°E).

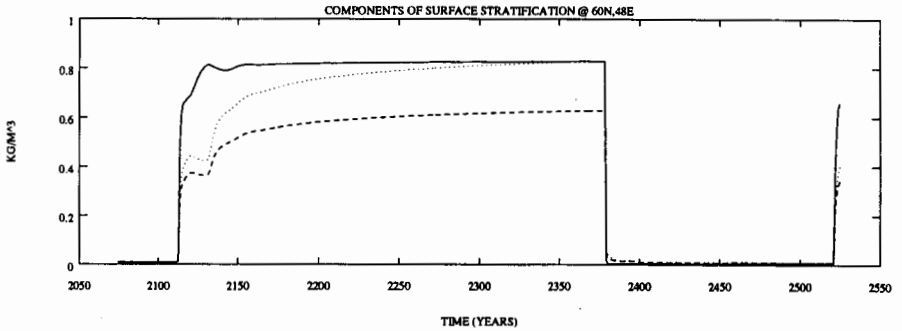

Figure 4: Components of the stratification between the upper two levels (25 m and 87.5 m) over the decoupled phase: linear stabilizing effect of the salinity gradient (solid); linear destabilizing effect of the temperature gradient (dashed). The linear effects are estimated with haline and thermal expansion coeffecients applicable late in the cold, coupled phase. The dotted line is the full destabilizing effect of temperature estimated as the linear haline stability minus the total stability. The increasing distance between the dotted and dashed lines represents the increasing destabilizing effect of non-linearity in the equation of state as the temperature increases over the decoupled phase.

It is perhaps unsurprising that sufficient freshening of the polar ocean surface can overcome the destabilizing effect of the heat transport beneath surface cooling to inhibit convection and halt the deep overturning. A more difficult task is to understand the processes which change the situation to favor renewed convection. There are no obvious changes in the circulation that would explain this in the current oscillation. The cyclonic gyre circulation is weakening near the surface just before convection breaks out. There is some sinking associated with the diffusive heat loss but it is not strong enough to be an important influence on heat and salt transports. A factor which must be considered is the non-linearity of the equation of state. The thermal expansion coefficient for seawater increases significantly as the temperature increases while the haline expansion coefficient is relatively insensitive to temperature changes. As the polar ocean warms the destabilizing effect of a given vertical temperature gradient increases. A critical contribution of this effect to the oscillations is indicated by experiments with a model using the linear equation of state, (1f'). With this model no deep decoupling oscillations were observed. An experiment with 1.65 times standard salt fluxes gave a steady deep coupled circulation, increasing the forcing to 1.675 times standard yielded a permanent polar halocline and thermally indirect circulation. Oscillations with a linear equation of state have been found in the model of

WS. These oscillations maintained limited high latitude convection during the decoupled phase. The precise reason for this difference with the current model is unknown but is likely related to the different salt flux pattern, the no slip boundary condition, or the two in combination.

Figure 4 shows the components of the static stability between the first and second levels in the model grid at the location where convection first breaks out to terminate the decoupled phase. The temperatures and salinities have been recorded just before the calculation of convective adjustment is made in the timestep sequence. The solid line is the salinity contribution to stability estimated with a haline expansion coefficient appropriate for the local temperature and salinity just prior to the formation of the halocline. This rises sharply when the halocline forms but grows imperceptibly thereafter. The dashed line is the destabilizing contribution of the temperature gradient estimated with the thermal expansion coefficient for conditions just prior to halocline formation. This linear temperature effect steadily decreases the stability. The dotted line is the total destabilizing effect of temperature calculated as the estimated haline stability minus the total stability. The difference between the dashed and dotted lines represents the influence of non-linearity in the equation of state on reducing the static stability as the sub-surface warming progresses. It contributes about 25% of the thermal destabilization when convection eventually renews.

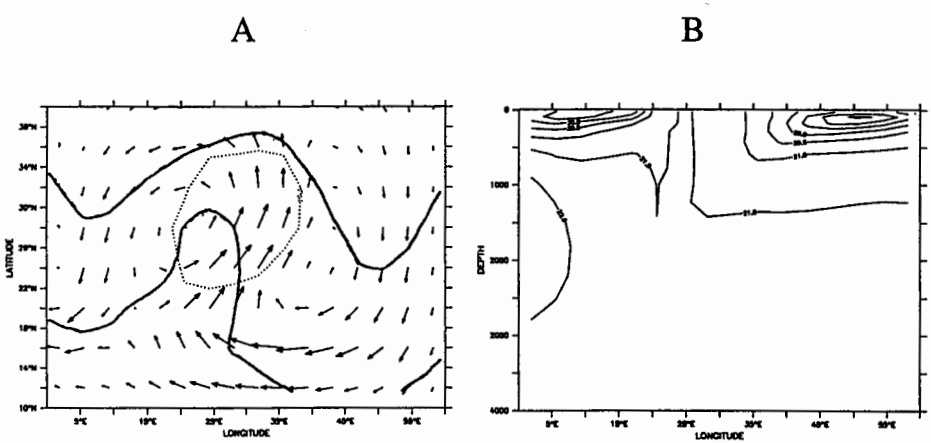

Figure 5: A convective eddy moving west to east across the basin in an experiment with the linear equation of state (1f') and 1.75 times the reference salinity forcing. (a) Circulation and salinity contours for 32 and 35 $kg \cdot m^{-3}$ (solid lines) at 87.5 m. The region inside the dotted contour has un upward surface heat flux greater than 20 $W \cdot m^{-2}$. (b) Zonal section of temperature through the eddy at 28°N.

Although no deep decoupling oscillations were observed with the linear equation of state another kind of oscillation with a decadal timescale is present in the experiments with a permanent polar halocline. Convecting patches form at regular intervals in the salty western boundary current of the subtropical gyre. In these patches, convection cools the water column and mixes salt up from the deep forming a dense core baroclinic vortex. This density is due to high salinities in the upper part and cool temperatures at depth. The vortices have a cyclonic circulation overlying an anti-cyclonic circulation (the opposite of a hurricane which has a light, warm core). The upper cyclonic flow advects heat and salt poleward on its eastern side, breaking down the halocline there, and moving the convection to the east. In this way the eddies propagate themselves eastward across the basin. The halocline reforms to the west of the eddies where strong southward surface velocities pull the halocline southward. As the deep ocean warms the eddies become more vigorous since they derive their energy from the density contrast between the core and the surrounding water. Figure 5a shows the cyclonic upper circulation an an eddy which has recently departed from the western boundary current and its deformation of the surface salinity field. The anti-cyclonic circulation to the east of the eddy is the undisturbed part of the subtropical gyre. The dense core of the eddy is shown in the zonal/vertical temperature section in Fig. 5b. The upper convecting region is on the eastern side of the deep cold core. Eddies of this kind were responsible for salting the polar region to terminate the decoupled period in the very strongly forced experiments of WS. They only seem to occur when the deep ocean is very warm (>15°C) and so are probably not relevant to the behavior of the natural ocean over the ice age cycles.

IV. A Three Box Halocline Oscillator

It is interesting to examine the interaction between convection and the non-linearity of the equation of state in a simpler context without dynamics and advective feedbacks. The three box model depicted in Fig. 6 is designed to represent the competing processes of upper level freshening and subsurface meridional heat transport. The low and high latitude surface boxes have fixed temperatures and a fixed "atmospheric" salinity flux from the high latitude to the low latitude box is imposed. There is horizontal mixing between the surface boxes (note that this only influences salinity) and vertical mixing with the deep box. When either of the low or high latitude water columns becomes unstable, the corresponding vertical mixing parameter is increased by a given factor to represent convective mixing. The equation of state has a non-linear dependence upon temperature (see eqn. 3f). The equations for the three box model are (refer to Fig. 6 for notation):

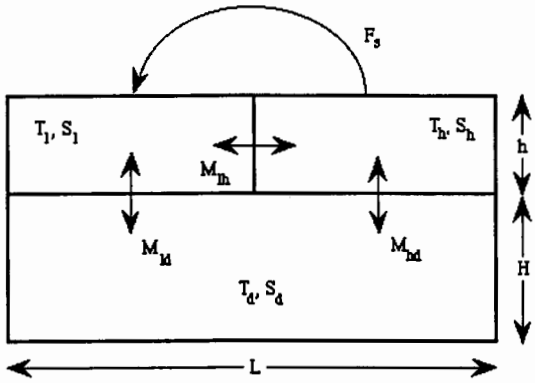

Figure 6: The three box model. Temperatures of the high and low latitude boxes are fixed and there is a fixed flux of salinity from the high to the low latitude box. Vertical mixing is increased when either of the low or high latitude water columns becomes gravitationally unstable.

$$\frac{dS_l}{dt} = \frac{2M_{ld}}{hL}(S_d - S_l) + \frac{2M_{lh}}{hL}(S_h - S_l) + \frac{F_s}{h} \tag{3a}$$

$$\frac{dS_h}{dt} = \frac{2M_{hd}}{hL}(S_d - S_h) + \frac{2M_{lh}}{hL}(S_l - S_h) - \frac{F_s}{h} \tag{3b}$$

$$\frac{dS_d}{dt} = \frac{M_{ld}}{HL}\left(S_l - S_d\right) + \frac{M_{hd}}{HL}\left(S_h - S_d\right) \tag{3c}$$

$$\frac{dT_d}{dt} = \frac{M_{ld}}{HL}\left(T_l - T_d\right) + \frac{M_{hd}}{HL}\left(T_h - T_d\right) \tag{3d}$$

$$M_{\{l,h\}d} = C_{\{l,h\}}M_v \tag{3e}$$

The convective parameters $C_{\{lh\}}$ are raised from 1 to 10 if $\rho(T_{\{lh\}},S_{\{lh\}})>\rho(T_d,S_d)$ where,

$$\rho(T,S)=0.79S-0.0611T-0.0055T^2. \tag{3f}$$

This equation of state is a quadratic fit to σ_θ between 0°C and 15°C. The next step is to choose

parameter values based upon the oscillations discussed in the previous section. For the geometry we choose h=50 m corresponding to the thickness of the top grid layer in the three dimensional model, H=500 m corresponding roughly to the thickness of the warm plume which moves into the high latitude ocean during the decoupled phase of the oscillations, and $L=6.37\cdot10^6$ m, the radius of the earth. T_l and T_h are fixed at 15°C and 0°C respectively. M_v is based upon a vertical diffusive timescale and M_{lh} is based upon mixing by Ekman drift in the three dimensional model so that:

$$\frac{HL}{2M_v} = 200\ years \approx \frac{H^2}{k_v}, \text{ and } \frac{hL}{2M_{lh}} = 5\ years \approx \frac{Lhf}{F_w}.$$

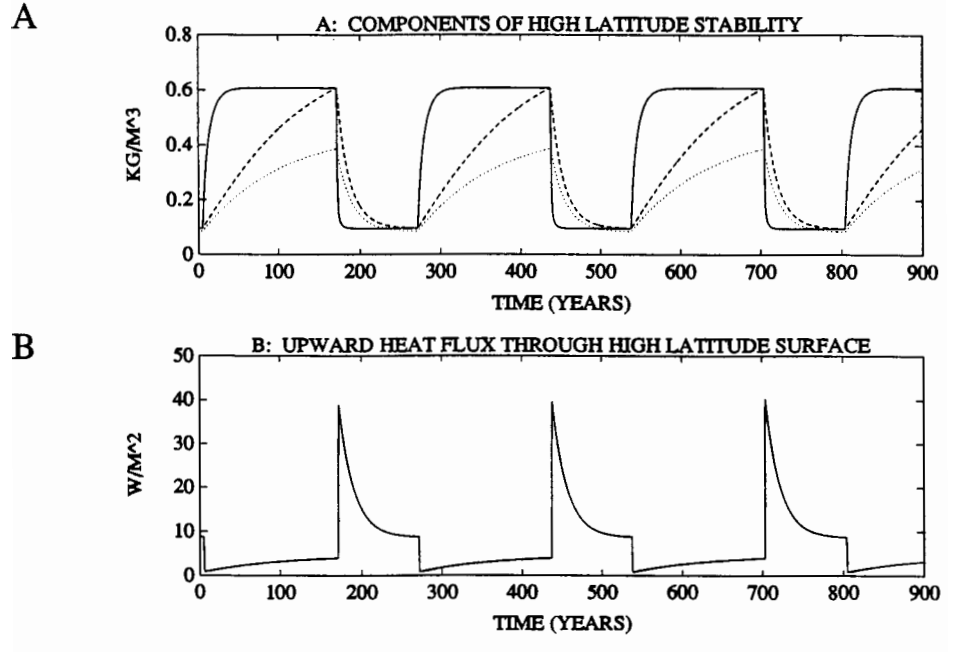

Figure 7: Three box model oscillations with $F_s=(-35\ kg\cdot m^{-3})\cdot(0.55\ m\cdot yr^{-1})$. (a) High latitude stability due to the vertical salinity gradient (solid), destabilizing effect of the vertical temperature gradient (dashed), and linear destabilizing effect of temperature estimated with the thermal expansion coefficient for 0°C (dotted); all in $kg\cdot m^{-3}$. (b) Upward heat flux through the high latitude surface ($W\cdot m^{-2}$).

With $F_s < 55$ cm·yr^{-1} the solutions are steady with a cold deep box and steady convection at high latitudes. For $F_s > 69$ cm·yr^{-1}, a permanent halocline prevents high latitude convection and the deep box temperature is the mean of the surface box temperatures. In between these two values, there are oscillations with non-convecting warming phases and convecting cooling phases (Fig. 7). The timescale for adjustment of the high latitude/deep salinity gradient is shorter than that for the temperature adjustment but the temperature gradient adjusts to a more extreme value. The lag makes the oscillations possible. A limit on the strength of the halocline during the non-convecting phase is imposed by horizontal mixing flux of salinity from the low latitude box to the high latitude box. The non-linearity of the equation of state ensures that the destabilizing effect of the temperature gradient will eventually fall below the stabilizing effect of the salinity gradient as the deep box temperature falls. In Fig. 7a the thermal destabilization can be seen catching up with the salt stabilization to switch convection on and off. The non-linearity in the equation of state increases the range of values taken by the thermal stabilization. Fig. 7b shows the upward heat flux through the polar surface over the oscillations. This flux is small during the stable phase but increases as the deep box warms. When convection resumes, the heat flux increases sharply. Falling deep temperature causes the convective heat flux to drop until the destabilizing effect of the temperature gradient is overwhelmed by the surface freshening and the heat flux drops sharply into the diffusive regime. In sensitivity experiments with increased salt fluxes, the oscillation period increased and the duration of the convective phase decreased until it was finally eliminated.

V. Discussion and Conclusions

The shape of the upward high latitude surface heat flux curve for the three box model is similar to that for oscillations of the three dimensional model (Fig. 8). In the later case, however, circulation changes enhance the convective changes. During the period of weak overturning the basin warms diffusively. When deep convection renews, a column of water is rapidly cooled by convective contact with the overlying boundary condition. Large meridional density gradients are set up which drive a large meridional overturning. The overturning harvests the heat which has accumulated during the decoupled phase and delivers it to high latitudes along with the heat from increased downward surface heat fluxes induced by cold upwelling. This subsurface heat transport beneath the cold surface boundary condition maintains convection during the coupled phase of the cycle. As the phase progresses, however, the basin cools and so both the overturning and heat flux weaken. Eventually surface freshening overcomes this weakened heat flux and a halocline catastrophe ensues. Large changes in the heat flux occur on a decadal timescale at phase transitions with a gradual decrease occurring throughout the coupled

phase. This cycle gives a high latitude surface heat flux curve which is similar to the temperature changes around the North Atlantic ocean over the Younger Dryas oscillation as shown schematically in a figure from Broecker (Broecker, 1991) redrawn here as Fig. 9. This shape has also been found in the Greenland ice core ^{18}O record of climate oscillations which occurred during the last glaciation (Johnson, 1992). The modelling results support the idea that the observed climate changes may be due to self sustaining cycles in the ocean's internal distribution of heat and salinity rather than to variations in salinity forcing as proposed by Broecker, et al. (1990). We might expect that sensitivity to forcing variations would depend upon the internal thermal structure prevailing at the time. Thus a meltwater pulse may not shut off convection when a deep thermocline is driving a large poleward heat transport. The timing and magnitude of the meltwater response to oceanic heat transport is a matter of primary interest for modelling these cycles.

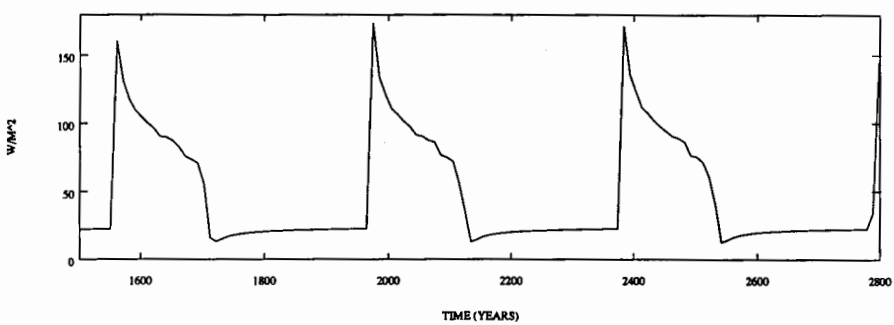

Figure 8: Upward surface heat flux (54°N to 70°N) over oscillations induced in the three dimensional model with 1.35 times the reference salt fluxes ($W \cdot m^{-2}$).

A simplified general circulation model with Laplacian friction and a no slip condition has reproduced the deep decoupling oscillations found in WS with a Rayleigh friction model. As in that study, it is found that during the deep decoupled phases of the oscillations, gyre circulations provide critical transports of heat and salt into the shallow polar ocean halocline and contribute to its eventual destabilization. A difference with the previous study is the presence of low amplitude oscillations which have no convection occurring in the polar ocean during the decoupled phase. This focuses attention upon role of the stratification in the upper polar ocean in the transitions between phases. Decoupling occurs after a period of reduced upward heat flux at high latitudes, halocline expansion, warmer and fresher sinking, and weakened overturning.

Three mechanisms contribute to the recoupling of the deep circulation. The first, most prominent in the Rayleigh friction study of WS, occurs when shallow convection and intermediate water formation are maintained in the polar ocean while the deep ocean is warming. In this case the convection and overturning strengthen and deepen gradually, importing more salt into the sinking regions. This process resembles a reverse halocline catastrophe in the mutually reinforcing effect of changes in circulation and salinity distribution. The second mechanism involves the direct destabilization of the polar stratification by rising subsurface temperatures without significant changes in the circulation over the decoupled phase. The non-linear dependence of density upon temperature in the equation of state is shown to play an important role in this process. Convecting eddies which depart from a salty western boundary current and propagate eastward through the polar halocline are a third method of switching on the deep overturning.

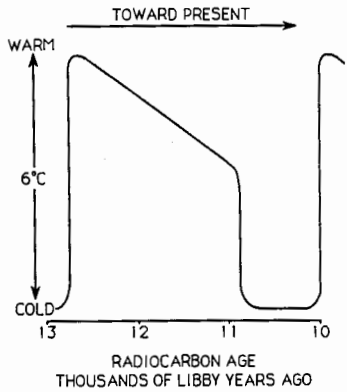

Figure 9: Schematic interpretation of temperature changes around the North Atlantic during the deglaciation by Broecker (redrawn from Broecker, 1991) based upon ^{18}O in ice and lake sediments, oceanic planktonic foraminifera, pollen, and beetles. See Broecker (1991) for references.

Acknowledgements

The author is grateful to Dr. E. S. Sarachik for comments on the manuscript. This work was supported by grants from the NSF and the NOAA/Office of Global Programs to the University of Washington Experimental Climate Forecast Center. This paper is JISAO contribution number 214.

References

Boyle, E. A., and Keigwin, L. D. (1987) North Atlantic thermohaline circulation during the past 20,000 years linked to high latitude surface temperature, *Nature*, **330**, 35-40.

Broecker, W. S. (1991) The great ocean conveyor, *Oceanography*, **4**, 79-89.

Broecker, W. S., G. Bond, M. Klas, G. Bonani, and W. Wolfi (1990) A salt oscillator in the glacial Atlantic? 1. the concept, *Paleoceanography*, **5**, 469-477.

Bryan, K., and M. D. Cox (1972) An approximate equation of state for numerical models of ocean circulation, *J. Phys. Oceanogr.*, **2**, 510-514.

Colin de Verdiere, A. (1988) Buoyancy driven planetary flows, *J. Mar. Res.*, **46**, 216-265.

Colin de Verdiere, A. (1989) On the interaction of wind and buoyancy driven gyres, *J. Mar. Res.*, **47**, 599-633.

Johnson, S. J., H. B. Clausen, W. Dansgaard, K. Fuhrer, N. Gundestrup, C. U. Hammer, P. Iverson, J. Jouzel, B. Stauffer, and J. P. Steffensen (1992) Irregular glacial interstadials recorded in a new Greenland ice core, *Nature*, **359**, 311-313.

Marotzke, J. (1989) Instabilities and multiple steady states of the thermohaline circulation. In: *Oceanic Circulation Models: Combining Data and Dynamics*, D. L. T. Anderson and J. Willebrand, Eds., NATO ASI series, Kluwer, 501-511.

Winton, M., and E. S. Sarachik (1993) Thermohaline oscillations induced by strong steady salinity forcing of ocean general circulation models, *J. Phys. Oceanogr.*, in press.